Controllable Wave Propagation of Hybrid Dispersive Medium with LC High-Pass Network

Author(s):
Parra, Edgar A.F.; Bergamini, Andrea E.; Ermanni, Paolo

Publication date:
2017

Permanent link:
https://doi.org/10.3929/ethz-a-010878241

Originally published in:
Proceedings of SPIE 10170, https://doi.org/10.1117/12.2258606

Controllable Wave Propagation of Hybrid Dispersive Medium with LC High-Pass Network

Edgar A. Flores Parra[a], Andrea Bergamini[b], and Paolo Ermanni[a]

[a]ETH Zürich, Composite Materials and Adaptive Structures Laboratory, Leonhardstrasse 21,CH-8092 Zürich Switzerland.

[b]EMPA, Materials Science and Technology, Laboratory for Mechanical Integrity of Energy Systems, Überlandstrasse 129, CH-8600, Dübendorf, Switzerland.

ABSTRACT

This paper reports on the wave transmission characteristics of a hybrid one dimensional (1D) medium. The hybrid characteristic is the result of the coupling between a 1D mechanical waveguide in the form of an elastic beam, and a discrete electrical network. The investigated configuration is based on an LC high-pass network. The capacitors are represented by a periodic array of piezoelectric elements that are bonded to the beam, coupling the mechanical and electrical domains, and thus the two waveguides. The coupling is characterized by a coincidence in frequency and wavenumber corresponding to the intersection of the dispersion curves. At this coincidence frequency, the hybrid medium features attenuation of wave motion as a result of the energy transfer to the electrical network. This energy exchange is depicted in the dispersion curves by eigenvalue crossing, a particular case of eigenvalue veering. This paper presents the numerical investigation of the wave propagation in the considered media, along with experimental evidence of the wave transmission characteristics. The LC high-pass network has the advantage of requiring a lower inductance value to achieve attenuation at the same frequencies as a low-pass network or local resonant shunt. The ability to conveniently tune the dispersion properties of the electrical network by varying the inductances is exploited to adapt the periodicity of the domain, i.e: monoatomic and diatomic unit cell configurations.

Keywords: Dispersion, piezoelectric, high-pass network, wave propagation

1. INTRODUCTION

There has been increased interest in the control of elastic waves with arrays of periodic piezoelectric shunts for attenuation of mechanical vibrations. Most of the past studies have focused on the reduction of structural vibrations with arrays of locally shunted piezoelectric elements[1–3] or grounded interconnected piezoelectric elements. This paper reports on a novel interconnection scheme for the unit cell of periodic structures, the LC high-pass (HP) network. As depicted in Fig. 1, floating piezoelectric elements are interconnected in series using grounded inductors, thus forming a high pass network. As will be shown in this article this extensions can have paramount effects on the overall dispersive properties of the resulting medium.

Forbidden frequency ranges in the dispersion curves of solid media through phononic crystals (PC) and mechanical metamaterials (MM) have been reported in literature. In PCs, bandgaps result from periodic modulations of the mass density and/or elastic constants[4,5] of the material resulting from the basis of the crystal (e.g. diatomic materials[6]). Such band gaps exist for wavelengths on the order of the unit cell size and can be complete,[7] namely for any direction of propagation, or partial, that is direction specific.[8] In metamaterials, on the other hand, the inclusion of suitably designed locally resonating units allows for the sub-wavelength modification of the dispersive properties of a medium, as reported amongst others by Liu in the mechanical domain.[9] Waves at frequencies corresponding to wavelengths substantially larger than the unit cell size can be attenuated by local resonators. Moreover, while periodicity is not strictly necessary to achieve wave attenuation in correspondence

Further author information: (Send correspondence to Edgar A. Flores Parra)
Edgar A. Flores Parra: E-mail: edgarf@ethz.ch, Telephone: 41-79-846-2573

with the tuning frequency of the resonator,[10] it is often assumed to allow for the calculation of its properties and dispersion curves. In both PCs and MMs, as reported in surveyed literature, waves propagate through the mechanical medium and interact with "inclusions" that either scatter them to generate destructive interference at certain wavenumbers, or that absorb and dissipate energy through local resonances. In many of the reported materials, the nature of the inclusions is purely mechanical.[7,9,11] In some cases, adaptive materials are exploited to modify the geometry of the unit cell,[12] to tune the properties of the locally resonating units[13–15] or to modify the connectivity of a PC.[16] In the latter cases, what could be defined as the electric domain of the unit cell is self-contained and only exchanges energy with the mechanical domain within the unit cell, thus it can be regarded as an inclusion in the mechanical medium. The mechanical component of the unit cell is thus the only pathway for the exchange of energy with neighboring cells.

Other interactions between mechanical and electrical modes can affect the propagation of waves leading to attenuation. As discussed by Mace et al.,[17] mode veering, and crossing, which can be considered a particular case of veering, occur due to weak eigenvalue coupling resulting in an exchange of energy between the modes. Crossing is the least common in literature and is more often discussed along with the veering phenomena. At crossing, the two modes exist at the same frequency, thus they are not uniquely defined, but can be described as the resultant of the two independent eigenvectors approaching the crossing point.[18]

This work considers macroscopic media made of "artificial atoms",[19] made of hybrid assemblies. The novelty of this contribution lies in the extension of the functionality of the atoms with connectivity in the electrical domain allowing simultaneous propagation of energy in the mechanical and electrical domains. The effect of electrical interconnection of the piezoelectric elements on the dynamic behavior of a structure has also been explored by dell'Isola et al.[20–23] to control multi-modal vibration damping through interconnected electrical resonators. In this contribution we will discuss the effect of the interaction between the electrical and mechanical modes on the propagation of transverse mechanical waves in the proposed HP network of the hybrid medium.

2. METHODOLOGY

The dispersion curves of the hybrid medium are calculated using numerical methods (FEM models implemented in COMSOL Multiphysics) by analyzing the eigenfrequencies of the unit cell modeled considering Floquet-Bloch boundary conditions. In the model of the one-dimensional hybrid medium periodic boundary conditions are applied to obtain $u_r = u_l e^{-\mathrm{i}ak}$, where u_r and u_l are respectively the mechanical degrees of freedom on the right and left side of the unit cell. For the electrical network periodicity is directly implemented using the *Global ODEs* and *DAEs* physics of COMSOL by imposing Eq. 5 which characterizes the HP network. Eq. 5 is derived by first relating the voltages V_{N-1},V_N and V_{N+1} across the piezoelectric elements to the current at node N. V_N, and the voltages across the adjacent piezoelectric elements V_{N-1} and V_{N+1} are related through the Floquet-Bloch boundary conditions given by Eq. 9 and 2. For the HP the relation between voltage and current in the unit cell leads to Eq. 3. L is the value of the inductor in the unit cell, k is the wavenumber, a is the lattice constant of the mechanical medium. Lastly, the voltage V_N is related to the charge Q on the top electrode of the piezoelectric element by $V_N = Q/C$, where C is the capacitance of the piezoelectric element. Time, t, is taken into account assuming harmonic oscillating charges $Q = q\sin(\omega t)$. Based on the latter assumption and Eq. 5, the dispersion relation for the HP network can be obtain, Eq. 10.

The transmittance calculation of the HP hybrid medium seen in Fig. 4b), is modeled using COMSOL Multiphysics. The dimensions of the modeled beam are 1 mm × 7 mm × 500 mm ($t \times w \times l$). Along the center portion of the structure, the hybrid medium with unit cell size of 10 mm is added. For the HP configuration 17 unit cells are positioned between 150 mm and 320 mm as seen in Fig. 2, whereas for the BP configuration 15 unit cells are placed between 150 mm and 300 mm. The beam material is 6061 aluminum alloy, while the piezoelectric element material is STEMiNC, SM111. The piezoelectric elements have a diameter d =7 mm and a thickness of t_p =0.4 mm yielding a capacitance value of around C =850 pF. The inductive and resistive components are modeled using the *electric circuit* physics of COMSOL. The mechanical transmittance of the finite hybrid medium is calculated by taking the ratio of the spatial average of the velocity amplitudes, over a region with 100 mm in length, before and after the periodic arrangement.

The experimental set-up for the HP configuration, seen in Fig. 2, was implemented using physical inductors. The monoatomic configuration used an inductance L =100 mH. The diatomic configuration of the HP used a

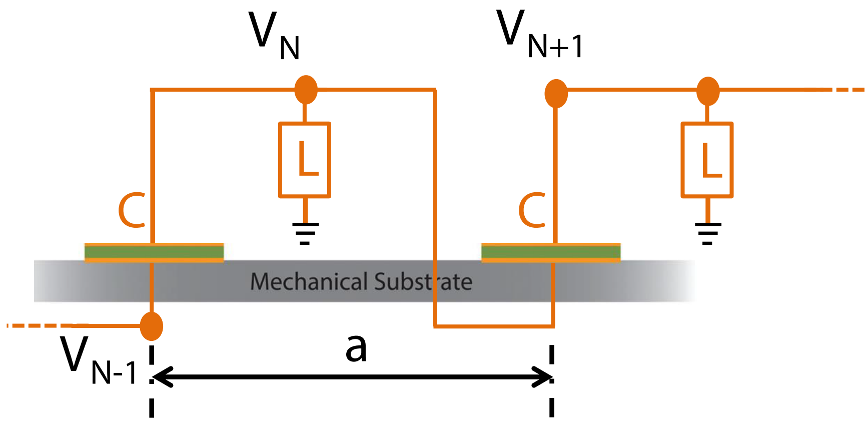

Figure 1. Unit cell HP

combination of L =100 mH and L =15 mH. All electrical components were arranged on a breadboard to facilitate reconfiguring the connections.

$$V_{N-1} = V_N e^{\mathrm{i}ak} \tag{1}$$

$$V_{N+1} = V_N e^{-\mathrm{i}ak} \tag{2}$$

$$C\left(\dot{V}_{N-1} - \dot{V}_{N+1} - 2\dot{V}_N\right) - \int \frac{V_N}{L} dt = 0 \tag{3}$$

$$V_N = Q/C \tag{4}$$

$$LC\ddot{Q}(e^{-\mathrm{i}ak} + e^{\mathrm{i}ak} - 2) - Q = 0 \tag{5}$$

$$\omega = -\frac{1}{2\sin(ak/2)\sqrt{LC}} \tag{6}$$

The wave attenuation capabilities of the HP hybrid medium can be further exploited by introducing a diatomic unit cell configuration. A diatomic unit cell can be designed by alternating both the capacitance or inductance values. In this case, a diatomic inductance configuration, described by Eq. 7 and 8, was investigated yielding the dispersion curves shown in Fig. 5a).

$$\ddot{Q}_1\left(e^{\mathrm{i}ak} + 1\right) - 2\ddot{Q}_2 - Q_2/(L_1 C) = 0 \tag{7}$$

$$\ddot{Q}_2\left(e^{-\mathrm{i}ak} + 1\right) - 2\ddot{Q}_1 - Q_1/\left(L_2 C\right) = 0 \tag{8}$$

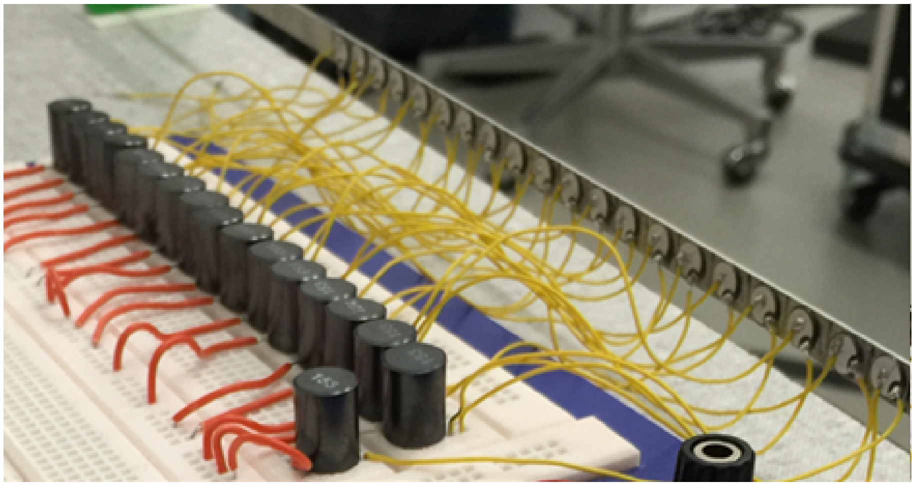

Figure 2. Experimental setup for monoatomic HP

3. RESULTS

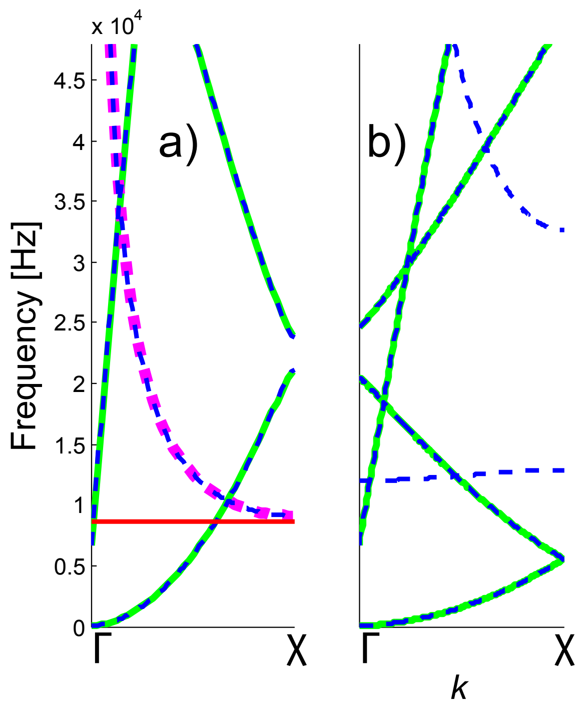

Figure 3. a) HP monoatomic dispersion for $L = 100\,\mathrm{mH}$, where the cut-ff frequency of the HP network is given by $f_{hp} = 1/(4\pi\sqrt{LC})$ and indicated by the red line, HP electrical mode (dotted magenta) b) Dispersion of diatomic HP network with $L = 100\,\mathrm{mH}$ and $L = 15\,\mathrm{mH}$

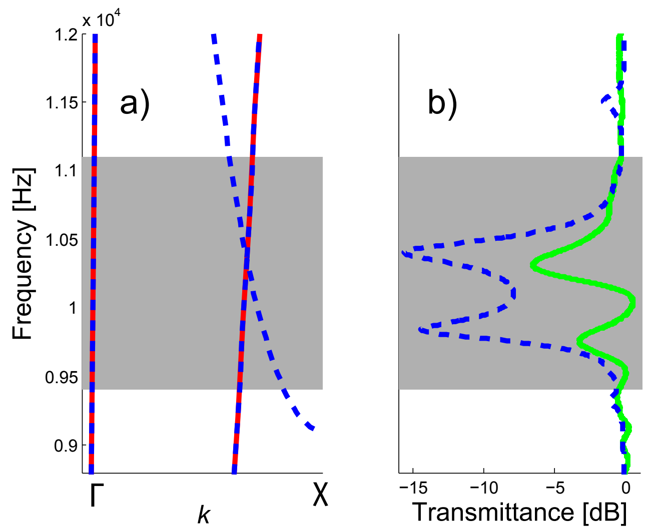

Figure 4. a) Mode crossing for monoatomic dispersion of HP with purely mechanical modes (solid red), and coupled modes (dotted blue) b) Numerical (dotted blue) and experimental (solid green) transmittance curves of the hybrid media for $L = 100\,\mathrm{mH}$

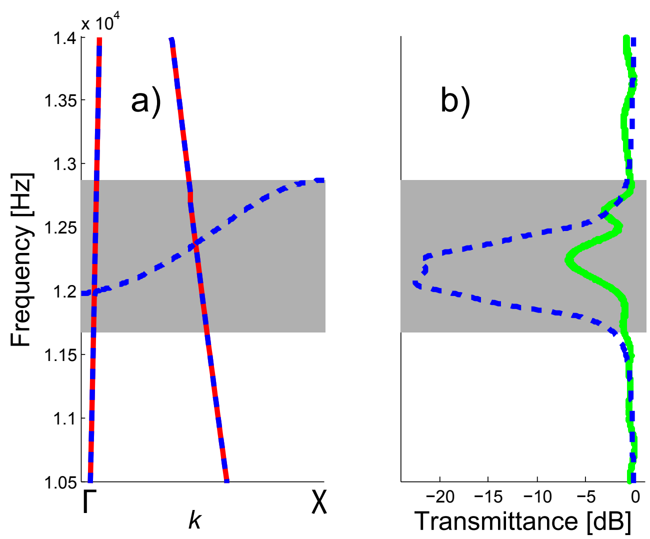

Figure 5. a) Mode crossing dispersion of first electrical mode of diatomic configuration with purely mechanical modes (solid red), and coupled modes (dotted blue) b) Numerical (dotted blue) and experimental (solid green) transmittance curves of the media for $L_1 = 100\,\mathrm{mH}$ and $L_2 = 15\,\mathrm{mH}$.

4. DISCUSSION

The dispersion of the HP monoatomic electrical mode, Fig. 3a), shows a medium where the phase velocity is positive while the group velocity is negative. The HP electrical mode displays an asymptotic behavior towards infinity as the wavenumber tends to zero, and convergence towards $f_{hp} = 1/(4\pi\sqrt{LC})$ as the wavenumber tends to the edge of the Brillouin zone. Moreover, as seen in Fig. 4a)-5a), eigenvalue crossing occurs at the intersections between the electrical and transverse mechanical modes for both the monoatomic and diatomic configurations. It is at the frequencies and wavenumber corresponding to crossing that attenuation occurs, indicating an exchange of energy between the mechanical and electrical domains. The attenuation can be seen in Fig. 4 b)-5b) where numerical and experimental results show a strong decrease in the transmittance at the crossing frequencies. Fig.

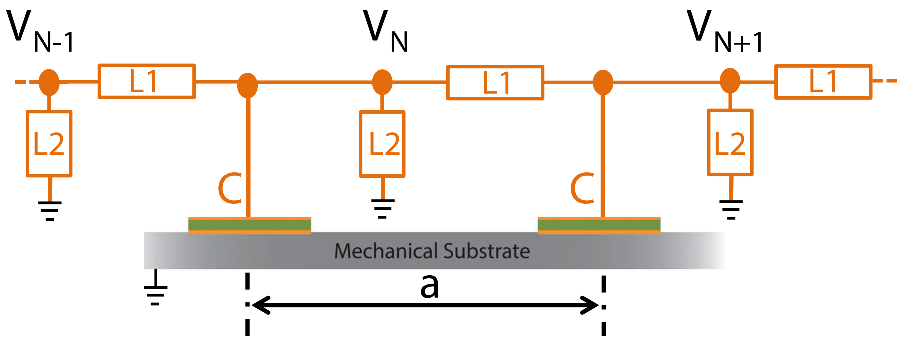

Figure 6. Unit cell of diatomic inductance BP

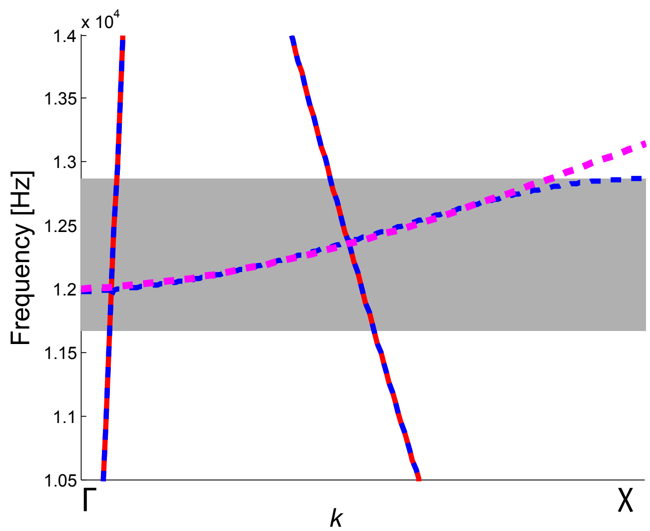

Figure 7. Mode crossing dispersion of first electrical mode of diatomic HP configuration with purely mechanical modes (solid red), and coupled modes (dotted blue). The electrical mode (magenta) of the diatomic inductance bandpass filter with L_1 =1000 mH, L_2 =100 mH, and C =1.76 nH is overlaid.

4b)-5b) show a good correlation between the experimental and numerical results in the frequency range over which attenuation occurs. However, the amplitude of the experimental results is significantly less than that of the numerical. This difference can be attributed to experimental conditions, such as the layer of glue at the interface between the piezoelectric elements and the substrate which diminishes the generalized coupling coefficient, and thus the effectiveness of the piezoelectric elements.

$$\frac{1}{L_1}\int (V_{N-1}-V_N)dt - \left(C\dot{V_N} + \int \frac{V_N}{L_2}dt\right) - \frac{1}{L_1}\int (V_N - V_{N+1})dt = 0 \tag{9}$$

$$\omega = \sqrt{\frac{e^{-\mathrm{i}ak}+e^{\mathrm{i}ak}-2}{L_1} - \frac{1}{L_2C}} \tag{10}$$

Fig. 3b) shows that two attenuation zones can be implemented with a diatomic HP unit cell. The diatomic configuration allows for tuning two independent attenuation zones using the same network. In the dispersion curves the diatomic HP configuration is characterized by the existence of two electrical modes. The higher frequency electrical mode has the same shape as that of the monoatomic HP configuration, while the electrical mode at the lower frequency, seen in Fig. 5a), has an S resembling that of a band-pass electrical mode.[24] The latter observation was corroborated by calculating the dispersion curves of a diatomic inductance band-pass (BP) network and comparing it to the first mode of the diatomic HP as illustrated in Fig. 6. Fig. 7, shows that for a given combination of inductances L_1, L_2, and piezoelectric elements with capacitance C the diatomic BP network has approximately the same shape as the first mode of the diatomic HP of Fig. 5a). The unit cell of the diatomic inductance BP network is depicted in Fig. 6.

5. CONCLUSION AND OUTLOOK

The HP interconnection scheme is one example of the myriad of networks that could be coupled with a mechanical waveguide to obtain variations of the hybrid medium with unusual wave propagation properties. Along with the low-pass and band-pass networks, the equations that describe the HP network remain relatively simple thus allowing for the calculation of their dispersion curves. Future work could focus of deriving the appropriate equations to implement richer and more complex discrete transmission lines. For example, the dual-composite right-left-handed (D-CRLH) transmission exhibits forward propagation at low frequencies, backward propagation at high frequencies, and no propagation in between the latter frequencies.

In the present work, we have shown the versatility of the HP interconnection scheme for generating areas of low mechanical transmittance by introducing an electrical waveguide through which energy can propagate, thereby attenuating transverse waves in their mechanical counterpart at the eigenvalue crossing frequencies. The rationale behind introducing a coupled electrical network lies in the ability to shape a systems mechanical response (characterized by its dispersion properties) without changing the mechanical layout. The HP offers an implementation where the piezoelectric elements do not need to be grounded and requires significantly smaller inductance values to achieve attenuation at the same frequency as the band-pass and low-pass networks[25] or the local resonant shunts. The HP diatomic configuration leads to two independent attenuation regions characterized by two separate electrical modes, one of which is similar the mode of a diatomic inductance band-pass network. By coupling a mechanical system to different electrical networks we have shown the dispersion properties of the hybrid medium can be tailored to achieve mechanical wave attenuation at one or multiple desired frequencies.

ACKNOWLEDGMENTS

This research was funded by the Swiss National Science Foundation Grant # 200021_157060. We thank our colleagues from the EMPA Acoustics/Noise Control Lab who provided support in carrying out the experimental testing.

REFERENCES

[1] Hollkamp, J. J., "Multimodal passive vibration suppression with piezoelectric materials and resonant shunts," *Journal of Intelligent Material Systems and Structures* **5**, 49–57 (1994).

[2] Beck, B. S., Cunefare, K. A., Ruzzene, M., and Collet, M., "Experimental analysis of a cantilever beam with a shunted piezoelectric periodic array," *Journal of Intelligent Material Systems and Structures* .

[3] Spadoni, A., Ruzzene, M., and Cunefare, K., "Vibration and wave propagation control of plates with periodic arrays of shunted piezoelectric patches," *Journal of Intelligent Material Systems and Structures* **20**, 979–990 (2009).

[4] Brillouin, L., [*Wave propagation in periodic structures: electric filters and crystal lattices*], Courier Corporation (1946).

[5] Deymier, P. A., [*Acoustic metamaterials and phononic crystals*], vol. 173, Springer Science & Business Media (2013).

[6] Krödel, S., Delpero, T., Bergamini, A., Ermanni, P., and Kochmann, D. M., "3d auxetic microlattices with independently controllable acoustic band gaps and quasi-static elastic moduli," *Advanced Engineering Materials* **16**(4), 357–363 (2014).

[7] Wu, T.-T., Huang, Z.-G., Tsai, T.-C., and Wu, T.-C., "Evidence of complete band gap and resonances in a plate with periodic stubbed surface," *Applied Physics Letters* **93**(11), 111902 (2008).

[8] Sato, A., Pennec, Y., Yanagishita, T., Masuda, H., Knoll, W., Djafari-Rouhani, B., and Fytas, G., "Cavity-type hypersonic phononic crystals," *New Journal of Physics* **14**(11), 113032 (2012).

[9] Liu, Z., Zhang, X., Mao, Y., Zhu, Y., Yang, Z., Chan, C., and Sheng, P., "Locally resonant sonic materials," *Science* **289**(5485), 1734–1736 (2000).

[10] Huang, H. and Sun, C., "Locally resonant acoustic metamaterials with 2d anisotropic effective mass density," *Philosophical Magazine* **91**(6), 981–996 (2011).

[11] Lee, J.-H., Singer, J. P., and Thomas, E. L., "Micro-/nanostructured mechanical metamaterials," *Advanced materials* **24**(36), 4782–4810 (2012).

[12] Robillard, J.-F., Matar, O. B., Vasseur, J., Deymier, P. A., Stippinger, M., Hladky-Hennion, A.-C., Pennec, Y., and Djafari-Rouhani, B., "Tunable magnetoelastic phononic crystals," *Applied Physics Letters* **95**(12), 124104 (2009).

[13] Airoldi, L. and Ruzzene, M., "Wave propagation control in beams through periodic multi-branch shunts," *Journal of Intelligent Material Systems and Structures* , 1045389X11408372 (2011).

[14] Casadei, F., Delpero, T., Bergamini, A., Ermanni, P., and Ruzzene, M., "Piezoelectric resonator arrays for tunable acoustic waveguides and metamaterials," *Journal of Applied Physics* **112**(6), 064902 (2012).

[15] Collet, M., Cunefare, K. A., and Ichchou, M. N., "Wave motion optimization in periodically distributed shunted piezocomposite beam structures," *Journal of Intelligent Material Systems and Structures* (2008).

[16] Bergamini, A., Delpero, T., Simoni, L. D., Lillo, L. D., Ruzzene, M., and Ermanni, P., "Phononic crystal with adaptive connectivity," *Advanced Materials* **26**(9), 1343–1347 (2014).

[17] Mace, B. R. and Manconi, E., "Wave motion and dispersion phenomena: Veering, locking and strong coupling effects," *The Journal of the Acoustical Society of America* **131**(2), 1015–1028 (2012).

[18] Kerschen, G., "Nonlinear dynamics: proceedings of the 32nd imac, a conference and exposition on structural dynamics, 2014. volume 2," in [*Conference proceedings of the Society for Experimental Mechanics series*], Berlin: Springer (2014).

[19] Lapine, M. and Tretyakov, S., "Contemporary notes on metamaterials," *IET microwaves, antennas & propagation* **1**(1), 3–11 (2007).

[20] Batra, R. C., DellIsola, F., Vidoli, S., and Vigilante, D., "Multimode vibration suppression with passive two-terminal distributed network incorporating piezoceramic transducers," *International Journal of Solids and Structures* **42**(11), 3115–3132 (2005).

[21] Maurini, C., Dell'Isola, F., and Del Vescovo, D., "Comparison of piezoelectronic networks acting as distributed vibration absorbers," *Mechanical Systems and Signal Processing* **18**(5), 1243–1271 (2004).

[22] Dell'Isola, F., Maurini, C., and Porfiri, M., "Passive damping of beam vibrations through distributed electric networks and piezoelectric transducers: prototype design and experimental validation," *Smart Materials and Structures* **13**(2), 299 (2004).

[23] Lossouarn, B., Deü, J., and Aucejo, M., "Multimodal vibration damping of a beam with a periodic array of piezoelectric patches connected to a passive electrical network," *Smart Materials and Structures* **24**(11), 115037 (2015).

[24] MartÃn, F., [*Artificial transmission lines for RF and microwave applications*], John Wiley & Sons (2015).

[25] Bergamini, A. E., Zündel, M., Parra, E. A. F., Delpero, T., Ruzzene, M., and Ermanni, P., "Hybrid dispersive media with controllable wave propagation: A new take on smart materials," *Journal of Applied Physics* **118**(15), 154310 (2015).